

# Spatio-temporal image correlation spectroscopy and super-resolution microscopy to quantify molecular dynamics in T cells

Ashdown, George W.; Owen, Dylan M.

DOI:

[10.1016/j.ymeth.2018.01.017](https://doi.org/10.1016/j.ymeth.2018.01.017)

License:

Creative Commons: Attribution-NonCommercial-NoDerivs (CC BY-NC-ND)

*Document Version*

Peer reviewed version

*Citation for published version (Harvard):*

Ashdown, GW & Owen, DM 2018, 'Spatio-temporal image correlation spectroscopy and super-resolution microscopy to quantify molecular dynamics in T cells', *Methods*, vol. 140-141, pp. 112-118.

<https://doi.org/10.1016/j.ymeth.2018.01.017>

[Link to publication on Research at Birmingham portal](#)

## **Publisher Rights Statement:**

Ashdown, W. & Owen, D. (2018) Spatio-temporal image correlation spectroscopy and super-resolution microscopy to quantify molecular dynamics in T cells, *Methods*, volume 140-141, pages 112-118, <https://doi.org/10.1016/j.ymeth.2018.01.017>

## **General rights**

Unless a licence is specified above, all rights (including copyright and moral rights) in this document are retained by the authors and/or the copyright holders. The express permission of the copyright holder must be obtained for any use of this material other than for purposes permitted by law.

- Users may freely distribute the URL that is used to identify this publication.
- Users may download and/or print one copy of the publication from the University of Birmingham research portal for the purpose of private study or non-commercial research.
- User may use extracts from the document in line with the concept of 'fair dealing' under the Copyright, Designs and Patents Act 1988 (?)
- Users may not further distribute the material nor use it for the purposes of commercial gain.

Where a licence is displayed above, please note the terms and conditions of the licence govern your use of this document.

When citing, please reference the published version.

## **Take down policy**

While the University of Birmingham exercises care and attention in making items available there are rare occasions when an item has been uploaded in error or has been deemed to be commercially or otherwise sensitive.

If you believe that this is the case for this document, please contact [UBIRA@lists.bham.ac.uk](mailto:UBIRA@lists.bham.ac.uk) providing details and we will remove access to the work immediately and investigate.

# Accepted Manuscript

## Spatio-Temporal Image Correlation Spectroscopy and Super-Resolution Microscopy to Quantify Molecular Dynamics in T cells

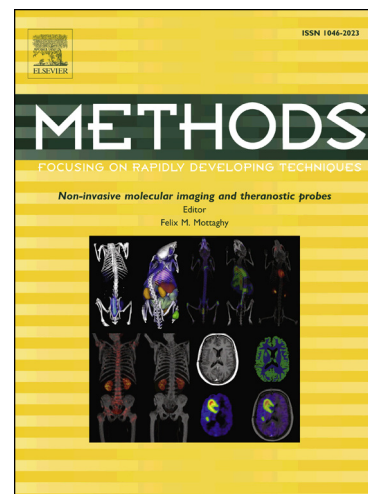
George W. Ashdown, Dylan M. Owen

PII: S1046-2023(17)30224-4  
DOI: <https://doi.org/10.1016/j.ymeth.2018.01.017>  
Reference: YMETHOD 4392

To appear in: *Methods*

Received Date: 15 November 2017  
Revised Date: 23 January 2018  
Accepted Date: 29 January 2018

Please cite this article as: G.W. Ashdown, D.M. Owen, Spatio-Temporal Image Correlation Spectroscopy and Super-Resolution Microscopy to Quantify Molecular Dynamics in T cells, *Methods* (2018), doi: <https://doi.org/10.1016/j.ymeth.2018.01.017>



This is a PDF file of an unedited manuscript that has been accepted for publication. As a service to our customers we are providing this early version of the manuscript. The manuscript will undergo copyediting, typesetting, and review of the resulting proof before it is published in its final form. Please note that during the production process errors may be discovered which could affect the content, and all legal disclaimers that apply to the journal pertain.

# **Spatio-Temporal Image Correlation Spectroscopy and Super-Resolution Microscopy to Quantify Molecular Dynamics in T cells**

George W. Ashdown<sup>a</sup>, Dylan M. Owen<sup>b\*</sup>

<sup>a</sup>Department of Life Sciences, Imperial College London, London, UK

<sup>b</sup>Department of Physics and Randall Division of Cell and Molecular Biophysics, King's College London, London, UK

## Abstract

Many cellular processes are regulated by the spatio-temporal organisation of signalling complexes, cytoskeletal components and membranes. One such example is at the T cell immunological synapse where the retrograde flow of cortical filamentous (F)-actin from the synapse periphery drives signalling protein microclusters towards the synapse centre. The density of this mesh however, makes visualisation and analysis of individual actin fibres difficult due to the resolution limit of conventional microscopy. Recently, super-resolution methods such as structured illumination microscopy (SIM) have surpassed this resolution limit. Here, we apply SIM to better visualise the dense cortical actin meshwork in T cell synapses formed against activating, antibody-coated surfaces and image under total-internal reflection fluorescence (TIRF) illumination. To analyse the observed molecular flows, and the relationship between them, we apply spatio-temporal image correlation spectroscopy (STICS) and its cross-correlation variant (STICCS). We show that the dynamic cortical actin mesh can be visualised with unprecedented detail and that STICS/STICCS can output accurate, quantitative maps of molecular flow velocity and directionality from such data. We find that the actin flow can be disrupted using small molecule inhibitors of actin polymerisation. This combination of imaging and quantitative analysis may

provide an important new tool for researchers to investigate the molecular dynamics at cellular length scales. Here we demonstrate the retrograde flow of F-actin which may be important for the clustering and dynamics of key signalling proteins within the plasma membrane, a phenomenon which is vital to correct T cell activation and therefore the mounting of an effective immune response.

Keywords: image correlation spectroscopy, structured illumination microscopy, cortical actin, T cell synapse.

\*Corresponding author dylan.owen@kcl.ac.uk

### **Introduction**

In many biological systems the key molecular species and interactions are well known. Many signalling proteins, for example, appear in a number of different signalling pathways. The question then arises as to how the cell regulates such signalling pathways and avoids potential cross-talk. In many systems, the answer seems to be via the complex spatio-temporal organisation of signalling molecules. Many proteins have well-defined organisation on spatial scales from nanometres to microns and on temporal scales from microseconds to minutes. Because of this, quantifying the spatial organisation of a protein and how that changes over time is a frequent goal in the biological sciences (1).

A classic example of this organisation is in T cells. In order to interrogate target cells for signs of infection, they form a highly-regulated signalling interface called the T cell immunological synapse (2, 3). Here, signalling proteins form microclusters containing tens of proteins and existing on the length scale of 10-100 nm. Such proteins include the T cell receptor (TCR) itself, kinases such as zeta-associated protein of 70 kDa (ZAP-70) and adaptor proteins such as linker for activation of T cells (LAT) (4). Actin forms a dense cortical meshwork at the periphery of the synapse which reduces in density towards the synapse centre; recent work using 3D-super resolution microscopy has demonstrated this meshwork exhibits a mean gap size of 200 nm(5). This research also demonstrates the difficulty in resolving individual fibres and gap sizes in the synapse periphery, which are frequently too dense to extract opening sizes or track fibres for flow speeds.

Previous research has quantified the temporal dynamics of this dense actin network, which is known to flow towards the synapse centre, using kymograph analysis (6, 7). Protein microclusters at the membrane also flow towards the synapse centre, where it is thought signalling is terminated. There is therefore a complex interplay of different forms of biophysically-driven protein spatio-temporal organisation regulating T cell signalling. However these previous methods are mostly limited to 1D quantification through time and rely on manually selecting subpopulations for tracking of user-defined structures to extract dynamic information.

One of the most common methods to study protein spatio-temporal organisation is fluorescence microscopy which offers molecular specificity and when optimised can be minimally invasive. For live cell imaging this optimisation takes the form of minimising the excitation laser power, by imaging a bright sample through fluorescent probe density or expression, while also generating conditions which reduce physiological stress such as protein overexpression. However, despite its advantages, fluorescence imaging has, until recently, remained limited in resolution by the diffraction of light. This means that the closest two objects can be is of the order of 200 nm. Since much spatial organisation exists on the scale of nanometres, this can make conventional fluorescence microscopy unsuitable. New fluorescence imaging methods that are capable of breaking the diffraction limit (so called 'super-resolution' techniques) include single-molecule localisation microscopy (SMLM) (8, 9), stimulated emission depletion microscopy (STED) (10) and structured illumination microscopy (SIM) (11). While SMLM is traditionally thought of as a slow acquisition, fixed-cell techniques, STED and SIM are capable of rapid imaging and therefore resolving molecular dynamics.

A number of statistical methods exist to analyse microscope image time-series and extract quantitative information on molecular dynamics such as diffusion and flow. These include algorithms such as particle tracking and dynamic masks which work well when individual objects, such as vesicles for example, can be identified in the image data. However, if there is no specific object or structure, fluorescence correlation approaches are frequently used.

Here, we will review one such method – spatio-temporal image correlation spectroscopy and its variants, and see how it can be applied to live-cell imaging data acquired by SIM.

### **Spatio-temporal image correlation spectroscopy**

In general, correlation approaches determine how quickly a signal is varying over space or time. Probably the most common implementation is fluorescence correlation spectroscopy (FCS) in which the time trace of detected fluorescence intensities is recorded over time from a stationary illumination spot, as molecules diffuse in and out of the volume (12). By performing an autocorrelation on the time-traces, it can be determined how long a fluorescent molecule spent in the illumination volume. This then gives the diffusion coefficient at a high temporal resolution but there is no spatial information and all data on the direction of molecular movement is lost. There are several extensions, notably scanning FCS where time-traces are recorded along a series of point positions (13). Originally an extension of scanning-FCS, image correlation spectroscopy (ICS) extended the power of using correlations spatially to both  $x$  and  $y$  dimensions simultaneously (14, 15). As whole sample fluorescence is observed simultaneously via a camera, it is suitable for both slower or quasi-static populations as well as sparse or densely packed molecules. Imaging data for ICS does however exhibit reduced temporal resolutions (0.1-10Hz), therefore ICS and its spatiotemporal variants are all based on correlating the fluctuations in fluorescence of individual pixels recorded through time and/or space. Both auto- and cross-correlations are required to extract this information.

As ICS methods sample the spatial dimension, analysis can also extract the immobile fluorescent populations, allowing them to be quantified or filtered out compared to classical FCS, with its exclusive time-domain.

During data acquisition, fluorescent signal is spread due to the diffraction of light through the microscope system. This spreading of emitted light is known as the point spread function (PSF) of the fluorophore and follows an approximately Gaussian distribution. As the goal of ICS is to correlate spatial measurements, it is vital to image the sample with a pixel size that is smaller than the diameter of the

PSF distribution. This will allow correlations to occur between neighbouring pixels and therefore improve the robustness of the correlation function.

After image acquisition, spatial ICS autocorrelates the data - that is each image is correlated with itself but with varying spatial shifts in  $x$  and  $y$ . This leads to the generation of a correlation function which represents the mathematical correlation of the image with itself (**Figure 1a**). An alternative correlative method akin to FCS is temporal ICS, where the same regions of an image (pixels) are autocorrelated through time (**Figure 1b**). The decay of the associated plot gives information on diffusion coefficients, flow speeds and immobile populations.

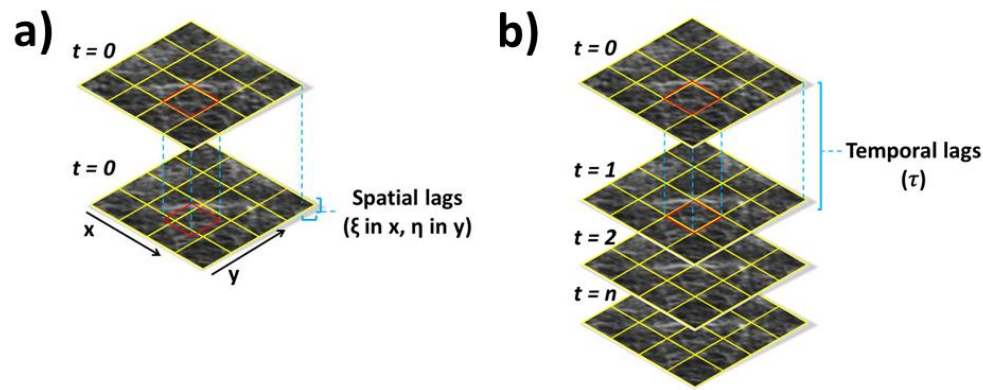


**Figure 1. Correlation of imaging data.** Spatial correlation of a dataset with itself (autocorrelation) at timepoint  $t$  will yield perfect correlation; by shifting the input image relative to the reference image by  $\xi$  and  $\eta$  results in a spatial correlation. Temporal correlation of imaging data, by correlating fixed spatial regions through multiple image slices correlations are plotted as a function of time.

ICS quantifies intensity fluctuations ( $\delta i$ ), defined as the difference in pixel intensity through time and space against the mean:

$$\delta i(x, y, t) = i(x, y, t) - [i]$$

Where  $\delta i$  signifies the difference between pixel intensity at a single point in space and time versus the mean intensity and  $[i]$  the average. This mean can define the spatial mean of a region of interest ( $x, y$ ) or the temporal mean for a single pixel through time ( $t$ ).

A limitation of FCS and ICS is their insensitivity to flow direction. However, combining spatial and temporal correlation techniques led to the development of spatiotemporal ICS (STICS) (16). The location of the correlation function peak within the correlative region gives information on both flowing and diffusive populations, where the flowing peaks location describes flow velocity.

$$G_{STICS}(\xi, \eta, \tau) = (\delta i[x, y, t] \delta i[x + \xi, y + \eta, t + \tau]_{xy}) t / [i]_t [i]_{t+\tau}$$

Where  $\xi$  and  $\eta$  are the spatial shifts and  $\tau$  the temporal lags. Denominator square brackets represent the mean intensities.

Spatial correlation at zero time lag ( $\xi, \eta, 0$ ) plots a correlation function centred at the origin (**Figure 2a**), as  $\tau$  increases and fluorescent populations diffuse (**Figure 2b**) or flow (**Figure 2c**), the peak will change shape and position from the centre. Diffusive populations can be separated from flowing signal as this peak stays central but increases in width (dependent on diffusion) as correlation occurs in all directions. These diffusive and static populations can be filtered out using techniques described in the next section.

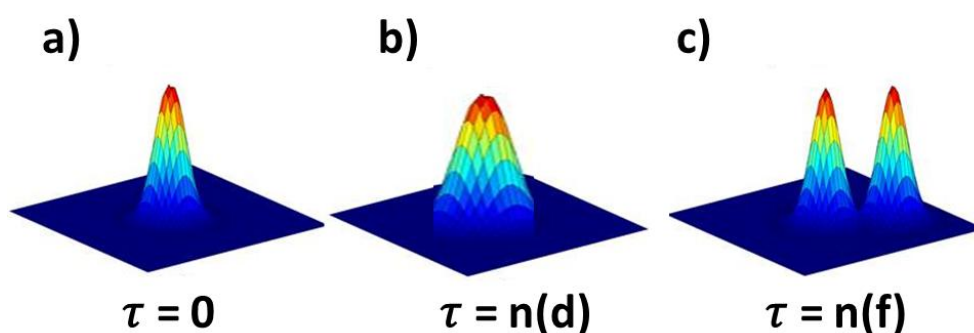


**Figure 2 Correlation function generation.** Upon correlation analysis, the output function generates different distributions, a) for spatial correlations at zero time lags ( $\tau = 0$ ) a function is centred at the origin, as  $\tau$  increases ( $\tau = n$ ) diffusive fluorescence will generate a wider Gaussian distribution (b), while populations that exhibit a net flow (c), the correlation function peak will change shape and position from the centre.

Net flow is detected as a Gaussian peak moving from the correlation function origin towards the periphery, where the height of the peak gives information on the density of the molecules while the distance and position relative to the origin signifies flow speed and directionality. This information on subregion flow speed



and directionality can then be represented with a vector map, where colour represents flow speed and orientation flow direction (**Figure 3**).

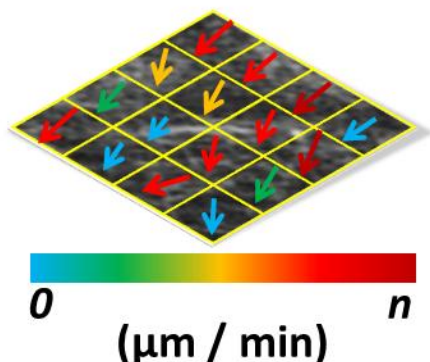


**Figure 3** Vector output representing flow dynamics. Subregion flow speed and directionality are represented as a vector map, where colour represents flow speed and orientation flow direction.

The magnitude of fluorescent fluctuation is inversely related to the number of detected emitters within the subregion; as such a concentration ceiling is set above which ICS techniques will break down. For cellular imaging where expression levels are relatively low (1-10 particles per beam focal area) this falls well below the  $\approx 100$  particle ceiling. Additionally, sample signal must also be balanced against signal to noise, where sample derived signal is required to be high enough for the ICS technique to reject spurious signal from the background.

ICS techniques provide advantages over other tracking and correlation methods but researchers must balance these against their limitations, outlined here. Correlation is assumed to take place in a 2D planar system, where flowing molecules make up at least 10% of the overall fluorescent population. Additionally, any immobile and diffusive objects that are present can obscure the flowing populations, as such ICS methods do require longer acquisitions and ideally higher signal fluctuations per subregion compared to traditional, point FCS. This represents a trade-off between correlating high numbers of fluctuations for a strong correlation function or sampling at faster rates to improve the temporal resolution. To ensure multiple emitters are correlated through multiple frames the dwell time between frames needs to be minimised.

Further, signal from the sample is assumed to originate from fluorophore dynamics, not photophysics or sample bleaching. Any 'blinking' from emitters or excessive bleaching can cause the correlation function to break down and increase spurious vector formation, which can be filtered out but at a loss of the sub-region during final quantification.

ICS techniques have been applied to fluorescent microscopy data from widefield using the total internal reflective fluorescence (TIRF) modality (17) and multi-photon/confocal systems (16). Each technique provides advantages depending on the sample being imaged; for faster biological processes widefield imaging provides continuous, whole sample illumination with each pixel reporting on fluorescent fluctuations simultaneously. Using TIRF ensures only emitters within the 100 nm evanescent wave from the coverslip-sample interface are excited, creating optical sectioning conditions and reducing photobleaching, aiding correlation function robustness. This does however limit the technique to imaging fluorophores residing within the depth of the evanescent wave.

Confocal and multi-photon imaging utilise a raster scanning approach to illuminate the sample with a focused beam of light. While these techniques can be slower to record larger regions of interest than widefield or TIRF illumination the focal point can be moved to anywhere within the sample, giving the researcher more flexibility. Additionally, the scanning technique can be employed to image subsections within the sample, leaving the rest of the specimen relatively unaffected. Whichever technique is used it is important to maintain optical sectioning, to reduce out of focus signal and obey the assumptions of the ICS software.

Recently Wavelet Imaging on Multiple Scales (WIMS) has been introduced(18), which are suited to multiple scaled events, such as simultaneously sampling cellular and molecular dynamics. This is an extension from correlation functions generated from Fourier transforms as with STICS, as it is capable of distinguishing between non-linear, complex systems. Additionally, when signal changes abruptly such as (for example, in fluorescent images) at the sample edge, Fourier analysis can break down, as the sine waves used do not localise in time or space. As

wavelets exist for a finite duration (unlike sine waves in Fourier transforms which oscillate infinitely), they can be used to localise discrete fluctuations.

Due to the discrete nature of the wavelets this analysis technique could also be used to extract multi-channel information occurring on different time scales, unlike STICS, this will allow clarification of whether dynamics are occurring within or outside specific regions of interest, such as structures including integrins.

### **Structured illumination Microscopy for use with STICS – Imaging considerations**

TIRF-SIM offers considerable advantages over conventional TIRF imaging for generating data for analysis by autocorrelation approaches. Not least STICS assumes the sample is 2D, so imaging with TIRF conditions improves analysis validity. However, some considerations when imaging live biological samples using SIM for STICS analysis should be highlighted.

Good signal-to-noise is crucial for multiple reasons<sup>(19)</sup>. Firstly, SIM reconstruction works optimally for structured signal; as such, images with less contrast can lead to reconstruction artefacts. This is also true for datasets where individual fluorophores translate between intensity maxima of the raw SIM data, leading to blurring and more diffusive signal during reconstruction. Depending on the speed of the dynamics being imaged, this will require minimising frame integration times so molecules are not lost out of the region of interest (ROI) before forming a correlation function. Slower sampling to collect enough information for image formation can therefore lead to artefacts in both the reconstructed data and correlation outputs.

As such, optimising both temporal and spatial resolutions depend on imaging a bright sample; if signal improvements from dimmer samples cannot be practically achieved by increasing the frame acquisition times, laser powers may need to be increased. For imaging live samples for prolonged time courses this requires careful considerations as phototoxicity can become an issue. The use of fluorophores with improved brightness can therefore reduce the requirements of longer frame acquisition times or sample perturbation from higher laser powers

through phototoxic effects. Datasets must also be long enough to allow any static or diffusive populations (manifested as a central peak of the correlation function) to be effectively separated from any flowing signal.

It should be noted, TIRF illumination has a substantial benefit when considering the above factors, through optical sectioning this modality can simultaneously improve signal-to-noise, reduce sample phototoxicity and improve photobleaching. As imaging with SIM requires the collection of 9 raw frames per reconstructed image, minimising photobleaching between acquisitions will lead to improved reconstructions and therefore correlation functions. Correlating greater spatial signal fluctuations per analysed subregion traditionally required increasing the correlation subregion size; however, this leads to a reduction in the spatial resolution of the output vector map. By instead reducing the pixel size, this limitation is circumvented. This allows researchers to retain or reduce subregion size, without reducing the strength of the correlation function, providing a greater amount of flow information per image, giving the potential to visualise sub-diffraction structures.

Finally, it is important to monitor specimen health, and maintain samples as close and consistently to culture conditions as possible. For this any media or solutions used for washing steps should be equilibrated to culturing temperatures, and for prolonged imaging schedules the microscope should be fitted with an environmental chamber to regulate heat and humidity. It is also good practice to handle cells as gently as possible before imaging, as any physiological or mechanical stress such as vigorous pipetting may lead to spurious results.

#### **Use of STICS software to analyse SIM data – analysis considerations**

After image acquisition the data can be analysed using an ICS software package. Here the STICS algorithm is described (16). Once the image is opened within the STICS software parameters can be optimised depending on the dataset. This section specifically deals with analysing TIRF-SIM data sets (20).

For samples with large amounts of immobile signal a filter based either on Fourier filtering of the zero-frequency components through time, or a sliding window subtraction (of adjustable length) of signal that remains static from each frame

should be used. Filtering removes the central peak of the correlation function associated with immobile populations, enabling more efficient mapping of flowing signal, by using the Fourier filter flow was quantified even when immobile signal reached 90% of the total. Another factor to consider is the subregion size and frame acquisition time, which when optimised can reduce spurious vector calculation and correlation artefacts. For subregion size, correlations can break down when imaging large structures or noisy data. As the STICS programme relies on correlating fluorescent fluctuations within each subregion, where the number of fluctuations inversely scales to the correlation function amplitude, it is important to increase these where possible and SIM data, with much smaller pixels is extremely effective for this purpose. Classically, this results in increasing the size of the subregion, thereby increasing the number of fluctuations per frame. Recently however, the combined use of super-resolution and image correlation approaches have provided enhanced correlation function generation through improved signal contrast. Both structured illumination and photoactivation localisation microscopy data has been analysed with STICS (21-23), which improves quantification due to smaller pixel sizes, this can reducing the ensemble effect of having excessive emitters within each subregions.

Regarding acquisition time, the number of frames needed is not as straightforward to determine with absolute precision. As an example, if the software detects 20 fluorescent proteins, all flowing in the same direction, fewer frames are required to generate a correlation function, however with fewer fluorophores, exhibiting less homogeneous flow the number of frames needed will increase. As such exact frame number and subregion size applied to the data will depend on the nature of the sample and the molecular events being imaged.

To ensure only valid fluctuations are correlated, outlier criteria are set – the beam radius thresholds out structures larger than the PSF of the microscope. When global image noise levels are similar to the height of the local correlation function these subregions are aborted using the correlation local maximum function. Additionally, when vector orientation deviates greatly from neighbouring vectors, these are also aborted through the vector mismatch threshold.

**Example data – Actin flow at the T cell immunological synapse**

To illustrate the use of structured illumination microscopy coupled with STICS analysis, we have analysed the retrograde flow of actin at the T cell immunological synapse. Jurkat T cells were transfected with LifeAct-GFP 24h prior to imaging via electroporation. Synapses were formed against glass coverslips coated with antibodies against the T cell receptor complex (cluster of differentiation 3 (CD3) and the co-stimulatory protein CD28 to induce activation (**Figure 4**).

Synapse forming T cells were imaged using a Nikon N-SIM microscope with TIRF illumination using 488 nm laser illumination set to 0.2 mW at the back focal plane. To maintain cell health during imaging cells were imaged within a heated chamber (Tokai Hit, Japan) fitted with a humidifier system and set to 37 °C. Images were acquired at 1 reconstructed frame per second with image stacks recorded for 1 minute.

Reconstruction took place within the NIS Elements Analyze software (v4.2, Nikon, Japan), achieving a pixel size of 30 nm and an image size of 1024 × 1024. The illumination pattern contrast (illumination modulation contrast, IMC) -which distinguishes stripes from the structured illumination pattern- and high resolution noise suppression (HRNS) -which crops out high resolution noise associated with SIM reconstruction- were both set to the default of 1. For the value of 1 this led to most of the higher frequency information remaining in the final image, for improved resolution.

After capturing F-actin dynamics using the N-SIM system (**Figure 4a**), STICS analysis confirmed the retrograde nature of the fluorescent signal through vector map outputs (**Figure 4b**), where red-shifted vectors demonstrate faster flow. **Figure 4c** demonstrates a montage of the reconstructed data where retrograde flow can be visualised by eye.

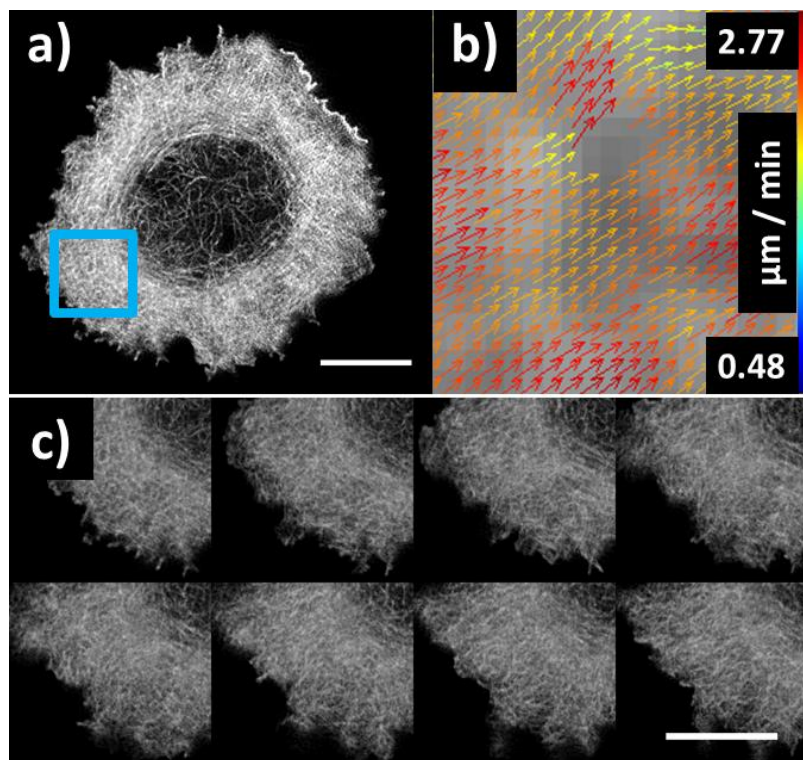


**Figure 4** Actin dynamics imaged using TIRF-SIM and analysed with STICS. **a)** F-actin in Jurkat T cell forming an immunological synapse is labelled by LifeAct-GFP, after STICS analysis, vector maps (**b**) are generated from selected ROI's in the distal region of cell synapse. An 8 frame montage is shown in **c**), running from top left to bottom right with increments of 5 frames. Scale bars = 5  $\mu\text{m}$ .

To further interrogate the T cell synapse, and in line with previous work (6, 24) actin-modulating drugs were added to quantify any changes in flow speed and directionality after perturbation. Following actin fibre disruption by the small molecule drug cytochalasin-D ( $2\mu\text{M}$ , **Figure 5a**), flow speeds ( $0.99 \pm 0.27 \mu\text{m}/\text{min}$ ) were significantly reduced ( $p < 0.001$ ) compared to controls ( $1.63 \pm 0.46 \mu\text{m}/\text{min}$ ). Additionally, actin retrograde flow (mean vector angle of  $40.8 \pm 23.35^\circ$ ) was significantly disrupted ( $p = 0.01$ ) compared to controls ( $63.7 \pm 21.0^\circ$ ).

Interestingly, T cells treated with the fibre stabilising drug jasplakinolide ( $2\mu\text{M}$ ) did not exhibit significant changes to flow speed ( $2.07 \pm 1.06 \mu\text{m}/\text{min}$   $p = 0.06$ ), but actin retrograde flow was significantly disrupted ( $61.1 \pm 27.5^\circ$   $p < 0.01$ ). These results are however, dose dependent – as demonstrated with results from previous studies showing actin flow reduced upon  $1 \mu\text{M}$  jasplakinolide



treatment(6) and in combination with myosin II inhibition with blebbistatin, in migrating keratocytes(25).

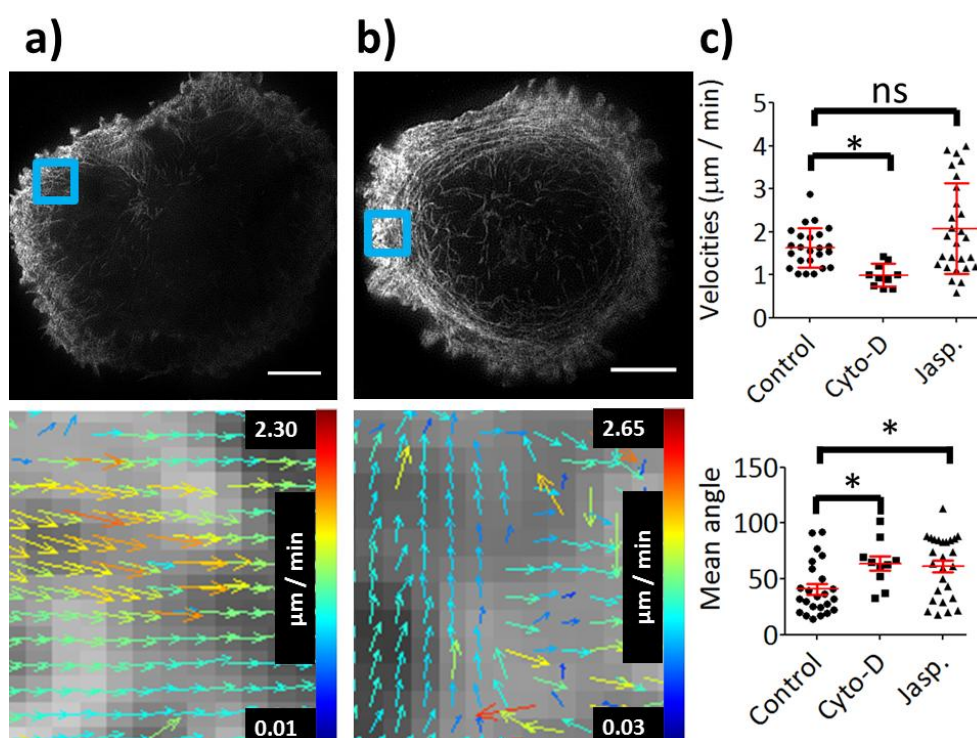


**Figure 5 Actin dynamics after drug perturbation.** T cells expressing LifeAct-GFP were treated with cytochalasin-D were imaged (a, top) and fluorescent signal quantified using STICS analysis (a, bottom), or treated with jasplakinolide (b). Flow dynamics could then be quantified compared to control data (c), here flow speeds and direction versus synapse centre are shown. Scale bars = 5 μm.

Together these results show that STICS analysis following TIRF-SIM data acquisition can capture the molecular dynamics of actin at the T cell synapse.

### **Conclusion**

Image correlation approaches such as STICS, are methods for extracting quantitative information on molecular dynamics from time-series of fluorescence microscopy data. This includes the determination of diffusion coefficients, flow velocities and flow directionality.

To improve the robustness of the generated correlation function requires the capturing of a greater number of fluorescent fluctuations; this has classically been achieved through increasing the correlated area at a cost to spatial resolution of



the analysed area. Here the combination of STICS and TIRF-SIM is demonstrated for the quantification of molecular scale dynamics within the context of the T cell synapse. By improving the resolution of the input images by a reduced pixel size more information per region of interest can be correlated, leading to robust correlative analysis within smaller regions of interest.

These results confirm F-actin polymerisation drives the dynamics of the retrograde flow seen during synapse formation and maintenance. Upon perturbation by small molecule drugs this flow speed is disrupted, leading to modulations in speed. Importantly, the additional information extracted from STICS analysis showed directionality is also disrupted. Modulating actin polymerisation reduced the retrograde nature of the flow within the dSMAC.

The combination of TIRF-SIM and STICS techniques could be applied to any biological sample exhibiting molecular flow and residing within the 200 nm evanescent wave of the coverslip-specimen interface. This could include investigating the nanoscale dynamics of cells undergoing migration or division or dynamics of labelling proteins or lipids residing close to or within the plasma membrane. The interplay between the actin cortex, the plasma membrane and membrane residing proteins is increasingly being investigated, as has been shown recently using both two-channel TIRF-SIM STICCS in T cells and single particle tracking in neurons respectively (22, 26).

#### Highlights

- Molecular-scale dynamics are important modulators of signalling pathways and processes
- Image correlation spectroscopy (ICS) permits the analysis of 2D images through time
- Combining ICS with structured illumination increases correlation robustness

- These techniques confirm the retrograde nature of F-actin within the T cell synapse
- Quantification of super-resolution data will be key for future use of these tools

### **Acknowledgements**

The authors acknowledge use of the Nikon Imaging Centre (NIC) at King's College London for use of the SIM microscope. We acknowledge Prof. Paul Wiseman and Dr Elvis Pandzic for the development of the STICS algorithm and software. We acknowledge funding from ERC starting Grant #337187.

### **References**

1. Lewitzky M, Simister PC, Feller SM. Beyond 'furballs' and 'dumpling soups' – towards a molecular architecture of signaling complexes and networks. *FEBS Letters*. 2012;586(17):2740-50.
2. Bromley SK, Burack WR, Johnson KG, Somersalo K, Sims TN, Sumen C, et al. The Immunological Synapse. *Annual Review of Immunology*. 2001;19(1):375-96.
3. Grakoui A, Bromley SK, Sumen C, Davis MM, Shaw AS, Allen PM, et al. The Immunological Synapse: A Molecular Machine Controlling T Cell Activation. *Science*. 1999 July 9, 1999;285(5425):221-7.
4. Saito T, Yokosuka T. Immunological synapse and microclusters: the site for recognition and activation of T cells. *Current Opinion in Immunology*. 2006 2006/6;18(3):305-13.
5. Fritzsche M, Fernandes RA, Chang VT, Colin-York H, Clausen MP, Felce JH, et al. Cytoskeletal actin dynamics shape a ramifying actin network underpinning immunological synapse formation. *Science Advances*. 2017;3(6).
6. Babich A, Li S, O'Connor RS, Milone MC, Freedman BD, Burkhardt JK. F-actin polymerization and retrograde flow drive sustained PLC $\gamma$ 1 signaling during T cell activation. *The Journal of Cell Biology*. 2012 June 11, 2012;197(6):775-87.
7. Beemiller P, Krummel MF. Mediation of T-Cell Activation by Actin Meshworks. *Cold Spring Harbor Perspectives in Biology*. 2010 September 1, 2010;2(9).
8. Betzig E, Patterson GH, Sougrat R, Lindwasser OW, Olenych S, Bonifacio JS, et al. Imaging Intracellular Fluorescent Proteins at Nanometer Resolution. *Science*. 2006;313:1642-5.
9. Rust MJ, Bates M, Zhuang X. Sub-diffraction-limit imaging by stochastic optical reconstruction microscopy (STORM). *Nature Methods*. 2006;3(10):793-6.
10. Hell SW, Wichmann J. Breaking the diffraction resolution limit by stimulated emission: Stimulated-emission-depletion fluorescence microscopy. *Optics Letters*. 1994 1 June 1994;19(11):780-2.

11. Gustafsson MGL. Surpassing the lateral resolution limit by a factor of two using structured illumination microscopy. *Journal of Microscopy*. 2000;198(2):82-7.
12. Elson EL, Magde D. Fluorescence correlation spectroscopy: Conceptual basis and theory. *Biopolymers*. 1974;13(1):1-27.
13. Ruan Q, Cheng MA, Levi M, Gratton E, Mantulin WW. Spatial-Temporal Studies of Membrane Dynamics: Scanning Fluorescence Correlation Spectroscopy (SFCS). *Biophysical Journal*. 2004 August 1, 2004;87(2):1260-7.
14. Petersen NO. Scanning fluorescence correlation spectroscopy. I. Theory and simulation of aggregation measurements. *Biophysical Journal*. 1986 April 1, 1986;49(4):809-15.
15. Petersen NO, Johnson DC, Schlesinger MJ. Scanning fluorescence correlation spectroscopy. II. Application to virus glycoprotein aggregation. *Biophysical Journal*. 1986 April 1, 1986;49(4):817-20.
16. Hebert B, Costantino S, Wiseman PW. Spatiotemporal Image Correlation Spectroscopy (STICS) Theory, Verification, and Application to Protein Velocity Mapping in Living CHO Cells. *Biophysical Journal*. 2005 May 1, 2005;88(5):3601-14.
17. Brown CM, Hebert B, Kolin DL, Zareno J, Whitmore L, Horwitz AR, et al. Probing the integrin-actin linkage using high-resolution protein velocity mapping. *Journal of Cell Science*. 2006 December 15, 2006;119(24):5204-14.
18. Toplak T, Palmieri B, Juanes-García A, Vicente-Manzanares M, Grant M, Wiseman PW. Wavelet Imaging on Multiple Scales (WIMS) reveals focal adhesion distributions, dynamics and coupling between actomyosin bundle stability. *PLoS ONE*. 2017;12(10):e0186058.
19. Demmerle J, Innocent C, North AJ, Ball G, Müller M, Miron E, et al. Strategic and practical guidelines for successful structured illumination microscopy. *Nature Protocols*. 2017 04/13/online;12:988.
20. Ashdown G, Pandzic E, Cope A, Wiseman P, Owen D. Cortical Actin Flow in T Cells Quantified by Spatio-temporal Image Correlation Spectroscopy of Structured Illumination Microscopy Data. *Journal of Visualized Experiments*. 2015 2015/12/17/(106):e53749.
21. Ashdown George W, Cope A, Wiseman Paul W, Owen Dylan M. Molecular Flow Quantified beyond the Diffraction Limit by Spatiotemporal Image Correlation of Structured Illumination Microscopy Data. *Biophysical Journal*. 2014;107(9):L21-L3.
22. Ashdown GW, Burn GL, Williamson DJ, Pandžić E, Peters R, Holden M, et al. Live-Cell Super-resolution Reveals F-Actin and Plasma Membrane Dynamics at the T Cell Synapse. *Biophysical Journal*. 2017;112(8):1703-13.
23. Pandžić E, Rossy J, Gaus K. Tracking molecular dynamics without tracking: image correlation of photo-activation microscopy. *Methods and Applications in Fluorescence*. 2015;3(1):014006.
24. Yi J, Wu XS, Crites T, Hammer JA. Actin retrograde flow and actomyosin II arc contraction drive receptor cluster dynamics at the immunological synapse in Jurkat T cells. *Molecular Biology of the Cell*. 2012 March 1, 2012;23(5):834-52.
25. Wilson CA, Tsuchida MA, Allen GM, Barnhart EL, Applegate KT, Yam PT, et al. Myosin II contributes to cell-scale actin network treadmilling through network disassembly. *Nature*. 2010 05/20/online;465:373.

26. Albrecht D, Winterflood CM, Sadeghi M, Tschager T, Noé F, Ewers H. Nanoscopic compartmentalization of membrane protein motion at the axon initial segment. *The Journal of Cell Biology*. 2016.

Highlights

- Molecular-scale dynamics are important modulators of signalling pathways and processes
- Image correlation spectroscopy (ICS) permits the analysis of 2D images through time
- Combining ICS with structured illumination increases correlation robustness
- These techniques confirm the retrograde nature of F-actin within the T cell synapse
- Quantification of super-resolution data will be key for future use of these tools

